THE JOURNAL OF PHYSICAL CHEMISTRY B

Article

pubs.acs.org/JPCB

# Folding of a Helix Is Critically Stabilized by Polarization of Backbone Hydrogen Bonds: Study in Explicit Water

Li L. Duan,[†,‡,§] Ya Gao,[†] Ye Mei,*[,†] Qing G. Zhang,[‡] Bo Tang,[§] and John Z. H. Zhang*[,†,∥]

[†]State Key Laboratory of Precision Spectroscopy, Department of Physics, and Institute of Theoretical and Computational Science, East China Normal University, Shanghai 200062, China

[‡]College of Physics and Electronics and [§]College of Chemistry, Chemical Engineering and Materials Science, Engineering Research Center of Pesticide and Medicine Intermediate Clean Production, Key Laboratory of Molecular and Nano Probes, Ministry of Education, Shandong Normal University, Jinan 250014, China

[∥]Department of Chemistry, New York University, New York, New York 10003, United States

**ABSTRACT:** Multiple single-trajectory molecular dynamics (MD) simulation at room temperature (300 K) in explicit water was carried out to study the folding dynamics of an $\alpha$-helix (PDB 2I9M) using a polarized charge scheme that includes electronic polarization of backbone hydrogen bonds. Starting from an extended conformation, the 17-residue peptide was successfully folded into the native structure ($\alpha$-helix) between 80 and 130 ns with a root-mean-square deviation of ~1.0 Å. Analysis of the time-dependent trajectories revealed that helix formation of the peptide started at the terminals and progressed toward the center of the peptide. For comparison, MD trajectories generated under various versions of standard AMBER force fields failed to show any significant or stable helix formation in our simulation. Our result shows clear evidence that the electronic polarization of backbone hydrogen bonds energetically stabilizes the helix formation and is critical to the stable folding of the short helix structure.

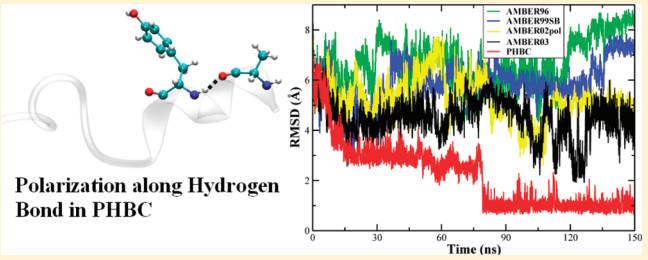


Intensive theoretical and experimental investigations have been performed over the years in attempts to understand the dynamics of protein folding from a random and extended state into its native structure.[1−4] Results from extensive experimental studies have provided many essential insights into the kinetics and thermodynamics of protein folding.[5,6] Along with experimental progress, theoretical and computational studies have played an indispensible role in increasing our understanding of protein folding at the atomic level. Theoretical folding studies have been performed at various levels of sophistication, ranging from simple lattice models to ab initio all-atom simulations in explicit water.[7−27] Ideally, it would be desirable to be able to predict the native structure of a protein ab initio on the basis of theoretical all-atom simulations. However, due to tremendous difficulties, successful direct ab initio protein folding has only been reported for a few small peptides.[10,27−30] Besides this, limitations in computer time and deficiencies in the force fields widely used for proteins also present a major obstacle to the successful folding of the vast majority of small proteins.[31]

One of the deficiencies in the force fields commonly used to study protein folding is a lack of electronic polarization. In standard nonpolarizable force fields, the partial atomic charges of the protein are prefixed regardless of the change in the electrostatic environment. Despite many efforts being devoted to development of the polarizable force field,[32] such a polarization effect on protein folding has not been well studied. Our recent work, which included the polarization effect in molecular dynamics (MD) simulations, demonstrated some important effects of electronic polarization on the structure and dynamics of proteins.[33−39] In this polarized protein-specific charge (PPC) approach, the partial atomic charges of proteins are determined from quantum chemistry calculations of proteins in solvents using a fragment approach.[33] Comparison of the simulation results with available experimental data showed that intraprotein polarization plays a significant role in stabilizing protein structure and dynamics. A similar conclusion was also reached by Gao and co-workers on the basis of a different theoretical approach with polarization.[40]

A major effect of polarization results from the electronic polarization of intraprotein hydrogen bonds. Recent studies[35] demonstrated that electronic polarization energetically stabilizes hydrogen bonds in proteins. Since hydrogen bonding is a prevalent feature in the structure of proteins, the stabilizing effect of a hydrogen bond has a significant impact on protein structure and dynamics.[41] In a recent ab initio folding study of a 17-residue peptide (PDB 2I9M),[42] the folding of the helix was completed in about 16 ns at room temperature. In this standard MD simulation, a polarization-adapted hydrogen-bond-specific charge scheme was used with an implicit solvation (generalized

**Received:** December 28, 2011
**Revised:** February 17, 2012
**Published:** February 27, 2012

  

Born, GB) model. In comparison, the MD simulation using the standard AMBER force field failed to fold the helix within the simulation time.[42] The work by Duan et al.[42] demonstrated the accelerating effect of hydrogen bond polarization on the formation of the helix.

However, the above work was performed using an implicit solvation (GB) model, which is inherently empirical in nature and does not exactly represent the real solvent effect. For example, hydrogen bonding between protein and water molecules is absent in the implicit solvation model. To examine the polarization effect of hydrogen bonds on helix formation in a real solvent, an MD simulation of helix formation in explicit water is necessary. In the present study, the polarization-adapted hydrogen-bond-specific charge (PHBC) scheme proposed in ref 42 was employed. In this PHBC scheme, the corresponding atomic charges of donors and acceptors of backbone hydrogen bonds, which are newly formed or broken, are refitted from fragment quantum mechanical calculations.

The 2I9M protein (amino acid sequence SAAEAYAK-RIAEAMAKG) was designed by Uceda et al. and folds spontaneously.[43] Recently, Lin et al.[44] employed a replica exchange molecular dynamics (REMD) simulation in an AMBER force field with GB implicit solvation[45] to study the folding of 2I9M. They found that it folds in 60 ns per replica, and this long folding time is due to the kinetic trap in a salt bridge formation that is absent in the native structure. Kim et al.[46] carried out a 60 ns (each replica) REMD simulation using a modified force field (param99MOD/GBSA). So far, to the best of our knowledge, there has been no report of a direct folding (single-trajectory or standard MD) simulation of 2I9M in explicit water. Here, we aimed to investigate the effect of hydrogen bond polarization on helix formation in explicit water. For this purpose, we carried out extensive standard MD simulations of 2I9M in explicit water at room temperature (300 K) using three slightly different versions of the PHBC scheme. In addition, MD simulation was also performed using various versions of the standard AMBER force field (AMBER96, AMBER99SB, AMBER02pol, and AMBER03) for explicit comparisons with the results obtained from the PHBC schemes.

## RESULTS AND DISCUSSION

**Single-Trajectory Result.** A standard MD simulation at room temperature (300 K) was carried out for a total of 150 ns under the PHBC scheme as well as under various versions of the AMBER force field. In the PHBC scheme, the standard AMBER03 force field was used for the peptide, but the atomic charges of any backbone hydrogen bond were dynamically updated from quantum calculations when the hydrogen bond was either newly formed or broken. The partial atomic charges of backbone hydrogen bonds are fitted from quantum calculations using RESP (restricted electrostatic potential) charge fitting.[47] The time development of the backbone rmsd (root-mean-square deviation) of the peptide (excluding terminal residues) is shown in Figure 1. The native structure is considered to be reached when the backbone rmsd is smaller than 1.5 Å.

First, let us examine the simulation result under standard AMBER force fields. As shown in Figure 1, the peptide did not show evidence of folding toward the native structure under standard AMBER force fields over the total simulation period of 150 ns. The rmsd generally fluctuated between 4.0 and 8.0 Å, and the intermediate structure that was closest to the native one

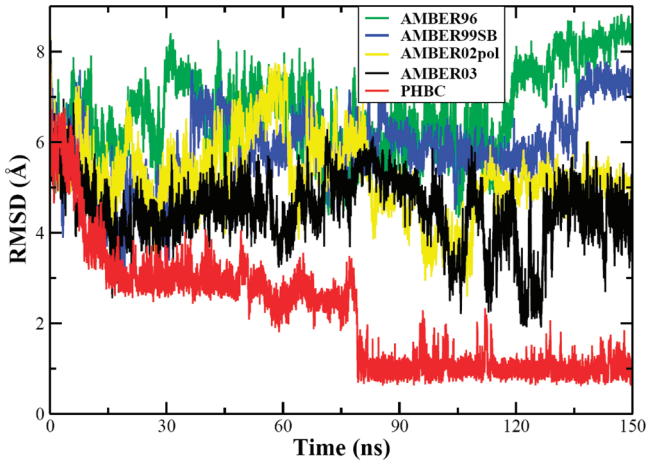


**Figure 1.** Root-mean-square deviations of backbone atoms of the peptide (2I9M) as a function of the MD simulation time using the AMBER96, AMBER99SB, AMBER02pol, AMBER03, and PHBC schemes.

was obtained in a standard AMBER03 force field, in which the rmsd of the peptide dropped close to 2.0 Å between 100 and 130 ns. In fact, an almost folded conformation was seen in the AMBER03 simulation, but these conformations were not stable, and the rmsd rapidly increased after 130 ns and fluctuated between 4.0 and 5.0 Å. An additional trajectory in the standard AMBER03 simulation showed a similar phenomenon; i.e., the peptide reached near native conformations for only a very short period of time and quickly changed to unfolded conformations.

It is noteworthy that the rmsd's from simulations under the AMBER96 and AMBER99SB force fields were much larger and hardly showed any evidence of folding. The rmsd from AMBER02pol, which included some polarization effects, was very similar to that from AMBER03. The above result indicates that the instantaneously formed helix was not energetically stable under the standard AMBER force field.

In comparison, the rmsd from the PHBC simulation showed clear evidence of folding, continuously dropping in steps of around 1.0 Å in about 80 ns and then stabilizing in subsequent MD simulations. An important feature in the PHBC simulation was that the rmsd continuously decreased without large fluctuations, in contrast to the large fluctuations of rmsd observed in the standard AMBER simulations, as shown in Figure 1. This is characteristic of a natural folding process in which the system simply follows the free energy path like in a funnel, as proposed by Onuchic and Wolynes.[2,48] This means that the protein is smart and folds itself straight down the free energy path without crossing over unnecessary barriers. Although the rmsd is shown in Figure 1 rather than the free energy, the underlying rationale and physical feature are similar.

If we further analyze the distribution of the rmsd from the PHBC simulation shown in Figure 2 in more detail, we can infer that the folding took place in four stages. The four most populous conformations had rmsd's of 5.5, 3.8, 3.0, and 1.0 Å at the corresponding time intervals shown in Figure 2. In the first stage (0−8 ns), the rmsd underwent a rapid fall from an initial value of 8.7 Å (extended structure) to around 5.5 Å. In this stage, the formation of the helix turn was initiated at two terminals of the peptide. This explanation is supported by Figure 3, which plots the time evolution of the peptide conformation. In the second stage (8−15 ns), the helix turns at two ends consolidated and progressed further toward the


dx.doi.org/10.1021/jp212516g | J. Phys. Chem. B 2012, 116, 3430−3435

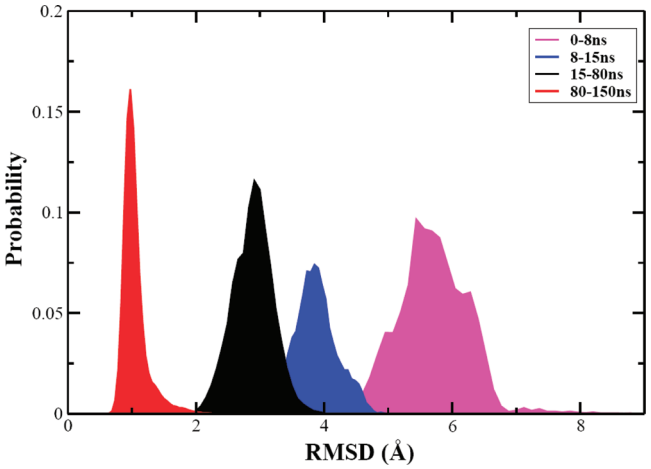


**Figure 2.** Distribution of the backbone rmsd's of 2I9M in the PHBC simulation during intervals of 0−8 ns (magenta), 8−15 ns (blue), 15−80 ns (black), and 80−150 ns (red). To calculate the distribution, 40 bins were constructed within each time interval. The backbone rmsd is given along the *x* axis, and the probability within each time interval is given along the *y* axis.

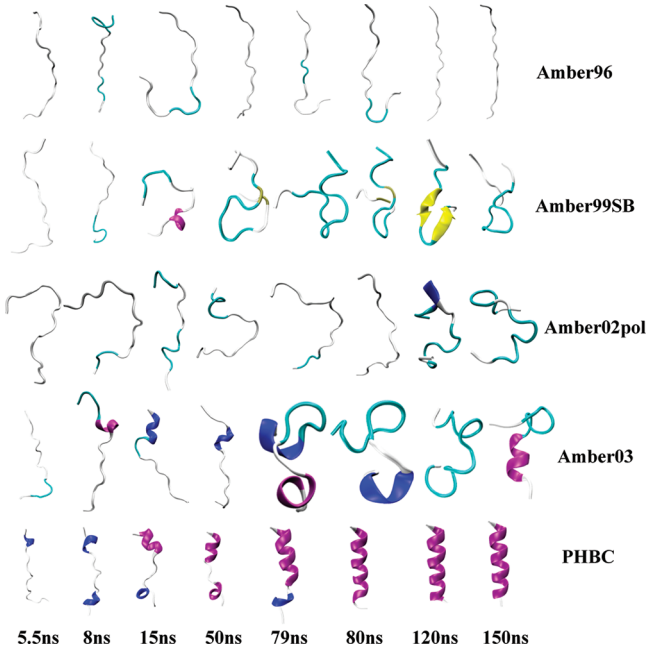


**Figure 3.** Snapshots of the intermediate conformations of the peptide at various simulation times using AMBER96, AMBER99SB, AMBER02pol, AMBER03, and PHBC. Here, the N terminal is always on the top. Key: α helix, purple; coil, white; turn, cyan.

center. In the third stage (15−80 ns), the progression of the helix turns toward the center continued and almost reached completion with an rmsd of around 2−3 Å. There was a rapid transition near 79−80 ns, representing completion of the last turn of the helix. This observation is consistent in both Figures 1 and 3. In the final stage (80−150 ns), the fully folded helix was stabilized with reasonable structural fluctuations.

It should be noted that the only difference between the PHBC and AMBER03 force fields was the partial atomic charges of backbone hydrogen bond donors and acceptors, whereas all of the other parameters of the force field were exactly the same. In the PHBC scheme, the atomic charges of the donor and acceptor of a backbone hydrogen bond were dynamically updated as the hydrogen bond was formed or broken. Thus, PHBC contained the electronic polarization effect of the hydrogen bond. Thus, significantly different folding results between PHBC and AMBER03 simulations should reflect this polarization effect or lack of it in the folding process. These results and analyses prove that electronic polarization of backbone hydrogen bonds (included in the PHBC simulation but not in the AMBER simulation) effectively accelerates formation of the helix by stabilizing the newly formed backbone hydrogen bonds and therefore leads the system down the minimum energy path without having to cross over unnecessary energy barriers.

To gain further insights into the intermediate states of the peptide at different stages of the folding process, we monitored its conformational changes during the MD simulation and plotted some representative conformations, as shown in Figure 3. These snapshots clearly show that no meaningful folding occurred during the MD simulations under various versions of the AMBER force fields during the entire simulation period. Among the various versions of AMBER, the result from AMBER03 was relatively better and showed partial folding of the helix during the process. This is consistent with the result from a previous study with a GB model.[42] In comparison, the simulation result using the PHBC scheme clearly showed a smooth folding process, with helix turns initially being formed at terminals and progressing toward the center. The rapid transition between 79 and 80 ns correlates with the completion of the last turn of the helix, and the complete formation of the helix took about 80 ns in our trajectory.

*Cluster Analysis, Native Contacts, and Hydrogen Bonds.* Figure 4 shows the representative structures for three of the

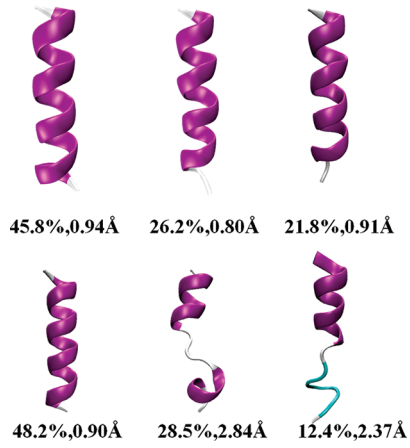


**Figure 4.** Representative conformations of the peptide selected from the most populated clusters in the PHBC simulation at 80−150 ns (top) and 0−150 ns (bottom). The populations of the clusters and the backbone rmsd's of the cluster centers are indicated.

most populated clusters during two simulation stages (80−150 ns, upper panel; 0−150 ns, lower panel). During the period of 80−150 ns, the rmsd fluctuated within 1.0 Å in three of the most populated clusters, with an overall population of 93.8%. This indicates that folding was completed and that the helix was generally stable.

The statistical distribution of the fractional native contacts over the entire simulation period in both AMBER and PHBC simulations is plotted in Figure 5. A native contact is defined as


dx.doi.org/10.1021/jp212516g | J. Phys. Chem. B 2012, 116, 3430−3435

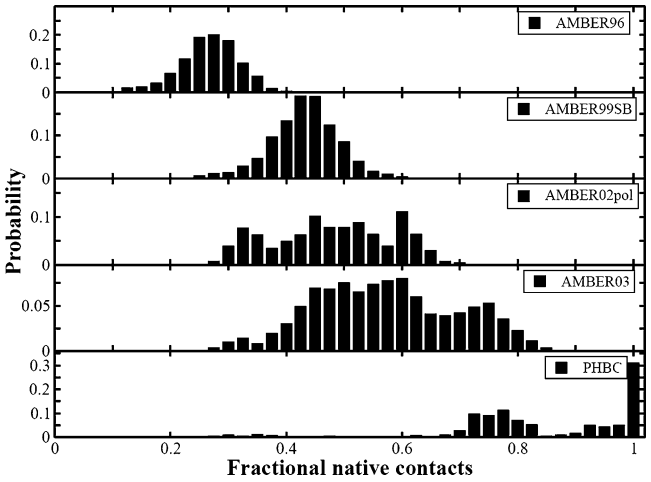


**Figure 5.** Statistical distribution of the fraction of native contacts over the entire simulation period under AMBER96, AMBER99SB, AMBER02pol, AMBER03, and PHBC force fields.

a contact in which the Cα−Cα distance is smaller than 7.0 Å for nonadjacent residues. There were a total of 39 native contacts in the first NMR (nuclear magnetic resonance) structure. The fractional native contact was defined as the number of total native contacts in a given conformation divided by the total number of native contacts in the NMR structure. The heavily populated states only had about 30%, 40%, 40−60%, and 50−60% of the native contacts in the AMBER96, AMBER99SB, AMBER02pol, and AMBER03 force fields, respectively, whereas in the PHBC simulation the most heavily populated states showed fractional native contacts in the range of 70−80% and near 100%.

For analysis of the hydrogen bonds, the fraction of native backbone hydrogen bonds in the helix during MD simulation was averaged over a time period of 100 ps. A hydrogen bond is counted if the distance between the two heavy atoms (N and O in this case) is less than 3.5 Å and the angle of N−H−O is larger than 120°. There were a total of 173 backbone hydrogen bonds in the helix in 20 NMR structures with an average number of 8.65 in each NMR structure. The fractional number of hydrogen bonds is defined as the number of native backbone hydrogen bonds in the helix of a simulated conformation divided by 8.65. Obviously, the fractional number of hydrogen bonds (∼100%) in the PHBC simulation, which fluctuated within 80−100%, was much higher than those in AMBER96 (∼0%), AMBER99SB (∼10%), AMBER02pol (∼30%), and AMBER03 (∼30%). All of the backbone hydrogen bonds in the NMR structure were reproduced in the PHBC simulation.

*Dynamic Cross-Correlation Map (DCCM).* To gain further insight into coordinated or concerted dynamic motions during the folding process, the dynamic cross-correlation of the motions between atom pairs was analyzed.[49−53] The dynamic cross-correlation coefficient for displacement of the $(i, j)$ pair of Cα atoms is defined as[54]

$$C_{ij} = \frac{\langle \Delta \mathbf{r}_i \cdot \Delta \mathbf{r}_j \rangle}{\sqrt{\langle \Delta \mathbf{r}_i^2 \rangle \langle \Delta \mathbf{r}_j^2 \rangle}}$$

where $\Delta \mathbf{r}_i$ is the displacement from the mean position (averaged over the entire trajectory) of the $i$th Cα atom and the angular brackets represent the time average over the trajectory. The coefficient $C_{ij}$ ranges from −1 to +1. A positive coefficient indicates that the pair of atoms are moving in the same direction, whereas a negative value indicates that they are moving in opposite directions. For example, $C_{ij} = -1$ denotes a completely anticorrelated motion and $C_{ij} = +1$ denotes a completely correlated motion. The larger the absolute value of $C_{ij}$, the more correlated or anticorrelated the motions of the atomic pair.

Figure 6 plots the DCCM of the fluctuations of Cα trajectories generated from both the AMBER03 and PHBC

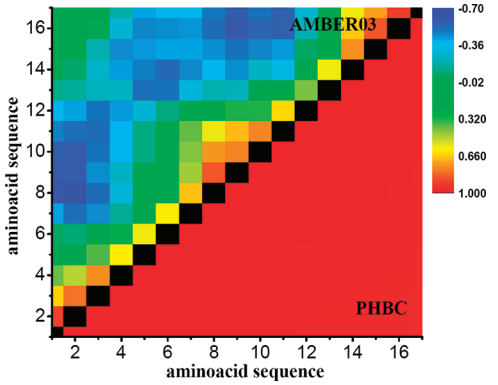


**Figure 6.** DCCM of the time-correlated atomic motions of Cα calculated over 150 ns from AMBER03 (upper left triangle) and PHBC (lower right triangle) simulations. A positive value indicates that the pair of atoms were moving in the same direction (correlated motion, in red), whereas a negative value indicates that the pair of atoms were moving in opposite directions (anticorrelated motion, in blue).

simulations. As shown in Figure 6, only very weakly correlated or concerted motions in the AMBER03 simulation were observed. Only the nearest residue pairs of 1−2, 2−3, 8−9, 15−16, and 16−17 showed highly correlated motions, whereas the other cross-correlation coefficients were very low. Also, about 58% of the anticorrelated motions were observed in the AMBER03 simulation. In contrast, the result from the PHBC simulation showed a strong, positive correlation with the correlation coefficient $C_{ij}$ within the range of 0.95−1, and no anticorrelated motions were found. *The strong correlation observed indicates that folding of the helix is a highly correlated dynamic process.* Highly cooperative structural dynamics is an important feature of successful folding in which a random population search in the conformation space is avoided. This is consistent with the funnel theory of Onuchi and Wolynes.[2,48] We note that some studies also emphasized the importance of cooperative interactions during the unfolding transitions of two-state systems.[55,56]

Because the PHBC simulation is computationally intensive due to the on-the-fly nature of quantum chemistry calculations, the MD simulation is only carried out for up to 150 ns, which is not sufficiently long for the statistical sampling of free energy; thus, a free energy analysis or mapping was not performed.

**Multiple-Trajectory Result.** A result based on one single-trajectory run using the PHBC scheme may not be sufficiently convincing to support the proposed mechanism that helix formation is accelerated by the polarization of backbone hydrogen bonding. Thus, two more trajectories were run using slightly different PHBC schemes (PHBC2 and PHBC3) to provide further data for analysis. The PHBC2 scheme differs from the PHBC scheme by determining whether the hydrogen bond is actually formed before charge fitting is performed. The


dx.doi.org/10.1021/jp212516g | J. Phys. Chem. B 2012, 116, 3430−3435

PHBC3 scheme is similar to the PHBC scheme except that charge fitting is based on a simpler quantum chemistry calculation. Further explanations of these two schemes are given in the Materials and Methods.

Figure 7 shows the time dependence of the backbone rmsd's from all three MD trajectories: PHBC, PHBC2, and PHBC3.

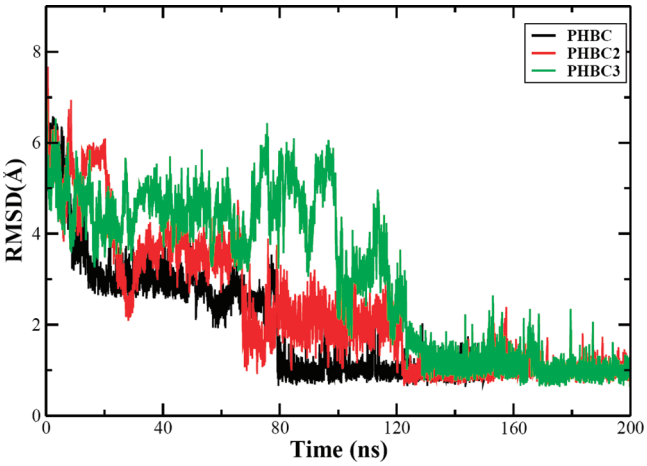


**Figure 7.** Root-mean-square deviations of backbone atoms of the peptide as a function of the simulation time in MD simulations using PHBC, PHBC2, and PHBC3.

As shown in this figure, the PHBC2 and PHBC3 trajectories reached the folded structure in 120 and 130 ns, respectively, which was somewhat longer than in the PHBC simulation. The total simulation time was also increased to 200 ns, confirming that the folded helix was stable. Although the details of the folding path and steps were not exactly the same in each individual trajectory, they generally conveyed very similar messages and were consistent with the mechanism proposed; i.e., the polarization of backbone hydrogen bonds accelerates the formation of helices by stabilizing backbone hydrogen bonds.

## CONCLUSION

In this work, a novel scheme (PHBC) was used to study the folding dynamics of a 17-residue peptide (2I9M) at room temperature in explicit water. The PHBC was derived from quantum mechanical calculations for the donors and acceptors of backbone hydrogen bonds and thus included the electronic polarization effect of hydrogen bonds. In the PHBC approach, the atomic charges of the relevant residues were fitted from quantum chemistry calculations based on the formation of backbone hydrogen bonds at regular time intervals during MD simulations. In multiple-trajectory PHBC simulations, starting from a fully extended conformation, 2I9M was successfully folded into an $\alpha$ helix within 80−130 ns with an rmsd of around 1 Å. With some reasonable structural fluctuations, the folded helix was generally stable.

In contrast, this peptide did not successfully fold into a complete helix when various versions of the standard AMBER force field were used in the MD simulations. Since only partial atomic charges of backbone hydrogen bond donors and acceptors were different in the PHBC and standard AMBER simulations, the difference in the folding results must have come from the relevant atomic charges that contained the proper polarization energy of the backbone hydrogen bonds. The systematic decrease in the rmsd over time and the highly correlated dynamic motion in the PHBC simulation were consistent with the expected folding pattern in which the protein follows the "smart" path without crossing high-energy barriers, as envisioned by the funnel theory of protein folding.[2]

## MATERIALS AND METHODS

We performed 150 ns MD simulations of 2I9M using the PHBC scheme and various versions of AMBER force fields (AMBER96, AMBER99SB, AMBER02pol, and AMBER03). Multiple trajectories using slightly different versions of the PHBC were also carried out for up to 200 ns. The fully extended initial structure was built by the Leap module in AMBER, and the simulations were carried out using the AMBER 10 simulation package.[57] In the MD simulation, the protein was placed in a truncated octahedral periodic box of TIP3P water. The distance from the surfaces of the box to the closest atoms of the solutes was set as 10 Å. Counterions were added to neutralize the system. The system was relaxed in a standard equilibration procedure. In the first step, only the solvent molecules were free to move, whereas the protein atoms were constrained by an external force. In the second step, the whole system was energy-minimized until convergence was reached. The system was then heated from 0 to 300 K over a period of 300 ps, and an MD simulation was performed in the NPT ensemble to further relax the system without any constraints on the solute atoms. Langevin dynamics,[58] with a collision frequency of 1.0 $ps^{-1}$, were applied to regulate the temperature, and the SHAKE algorithm[59] was employed to fix all of the bonds involving hydrogen atoms. The trajectory was saved every 1 ps, and these snapshots were used for detailed analyses.

In our on-the-fly MD simulation using the PHBC scheme,[42] atomic charges were initially taken from the AMBER03 force field, but the charges of donors and acceptors of backbone hydrogen bonds were periodically updated using the PHBC scheme. During the MD simulation, checks were periodically performed to determine whether any nascent backbone hydrogen bond had formed or an existing one had broken. If this was the case, the PHBC scheme described above was performed to update the atomic charges of the corresponding residues and the MD simulation was continued using the updated atomic charges. In the present simulation charge updates were carried out every 20 ps, which was found to be sufficient. More frequent updates would significantly increase the computational costs and show no significant differences in the results. In the modified PHBC2 scheme, the occupancy of the hydrogen bond was used as the criterion for determining whether the hydrogen bond was counted, instead of the instantaneous criterion used in PHBC. If the occupancy of a particular hydrogen bond was less than 30%, it was ignored. Changes in the hydrogen bonds were checked over a time period of 20 ps. The PHBC3 scheme was similar to the PHBC scheme except that the quantum chemistry calculation was performed at the HF/6-31G* level in the gaseous phase instead of DFT/B3LYB/6-31G* in the conductor-like polarizable continuum model.

## AUTHOR INFORMATION

### Corresponding Author

*E-mail: ymei@phy.ecnu.edu.cn (Y.M.); john.zhang@nyu.edu (J.Z.H.Z.).

## Notes

The authors declare no competing financial interest.

## ■ ACKNOWLEDGMENTS

L.L.D. is grateful to the National Natural Science Foundation of China (Grant 11147026) and the Scientific Research Award Fund for the Excellent Middle-Aged and Young Scientists of Shandong Province (Grant BS2011SW046) for support. Y.M. was supported by the Shanghai Rising-Star program (Grant 11QA1402000). Q.G.Z. thanks the National Natural Science Foundation of China (Grant 10874104) and the Research Fund for the Doctoral Program of Higher Education of China (Grant 20093704110001) for support. B.T. was supported by the National Key Natural Science Foundation of China (Grant 21035003) and the National Natural Science Funds for Distinguished Young Scholars (Grant 20725518). J.Z.H.Z. acknowledges financial support from the National Natural Science Foundation of China (Grants 10974054 and 20933002) and the Shanghai PuJiang program (Grant 09PJ1404000). We thank the Supercomputer Center of East China Normal University for CPU time support.

## ■ REFERENCES

(1) Dill, K. A.; Chan, H. S. *Nat. Struct. Biol.* **1997**, *4*, 10−19.
(2) Onuchic, J. N.; Luthey-Schulten, Z.; Wolynes, P. G. *Annu. Rev. Phys. Chem.* **1997**, *48*, 545−600.
(3) Alm, E.; Baker, D. *Curr. Opin. Struct. Biol.* **1999**, *9*, 189−196.
(4) Dobson, C. M.; Karplus, M. *Curr. Opin. Struct. Biol.* **1999**, *9*, 92−101.
(5) Fernndez-Escamilla, A. M.; Cheung, M. S.; Vega, M. C.; Wilmanns, M.; Onuchic, J. N.; Serrano, L. *Proc. Natl. Acad. Sci. U.S.A.* **2004**, *101*, 2834−2839.
(6) Yang, W. Y.; Gruebele, M. *J. Am. Chem. Soc.* **2004**, *126*, 7758−7759.
(7) Swendsen, R. H.; Wang, J. S. *Phys. Rev. Lett.* **1986**, *57*, 2607−2609.
(8) Berg, B. A.; Neuhaus, T. *Phys. Lett. B* **1991**, *267*, 249−253.
(9) Hansmann, U. H. E. *Chem. Phys. Lett.* **1997**, *281*, 140−150.
(10) Duan, Y.; Kollman, P. A. *Science* **1998**, *282*, 740−744.
(11) Duan, Y.; Wang, L.; Kollman, P. A. *Proc. Natl. Acad. Sci. U.S.A.* **1998**, *95*, 9897−9902.
(12) Zhou, R. H.; Berne, B. J.; Germain, R. *Proc. Natl. Acad. Sci. U.S.A.* **2001**, *98*, 14931−14936.
(13) Brooks, C. I. *Acc. Chem. Res.* **2002**, *35*, 447−454.
(14) Daggett, V. *Acc. Chem. Res.* **2002**, *35*, 422−449.
(15) Simmerling, C.; Strockbine, B.; Roitberg, A. *J. Am. Chem. Soc.* **2002**, *124*, 11258−11259.
(16) Pande, V. S.; Baker, I.; Chapman, J.; Elmer, S. P.; Khaliq, S.; Larson, S. M.; Rhee, Y. M.; Shirts, M. R.; Snow, C. D.; Sorin, E. J.; Zagrovic, B. *Biopolymers* **2003**, *68*, 91−109.
(17) Pitera, J. W.; Swope, W. *Proc. Natl. Acad. Sci. U.S.A.* **2003**, *100*, 7587−7592.
(18) Zhou, R. H. *Proc. Natl. Acad. Sci. U.S.A.* **2003**, *100*, 13280−13285.
(19) Juraszek, J.; Bolhuis, P. G. *Proc. Natl. Acad. Sci. U.S.A.* **2006**, *103*, 15859−15864.
(20) Wickstrom, L.; Okur, A.; Song, K.; Hornak, V.; Raleigh, D. P.; Simmerling, C. L. *J. Mol. Biol.* **2006**, *360*, 1094−1107.
(21) Baumketner, A.; Shea, J. E. *J. Mol. Biol.* **2007**, *366*, 275−285.
(22) Lei, H.; Wu, C.; Liu, H.; Duan, Y. *Proc. Natl. Acad. Sci. U.S.A.* **2007**, *104*, 4925−4930.
(23) Paschek, D.; Nymeyer, H.; Garcia, A. E. *J. Struct. Biol.* **2007**, *157*, 524−533.
(24) Scheraga, H. A.; Khalili, M.; Liwo, A. *Annu. Rev. Phys. Chem.* **2007**, *58*, 57−83.
(25) Yoda, T.; Sugita, Y.; Okamoto, Y. *Proteins: Struct., Funct., Bioinf.* **2007**, *66*, 846−859.
(26) Nelson, E. D.; Grishin, N. V. *Proc. Natl. Acad. Sci. U.S.A.* **2008**, *105*, 1489−1493.
(27) Lei, H.; Wang, Z.; Wu, C.; Duan, Y. *J. Chem. Phys.* **2009**, *131*, 165105.
(28) Ferrara, P.; Apostolakis, J.; Caflisch, A. *J. Phys. Chem. B* **2000**, *104*, 5000−5010.
(29) Yang, L.; Shao, Q.; Gao, Y. Q. *J. Phys. Chem. B* **2009**, *113*, 803−808.
(30) Shaw, D. E.; Maragakis, P.; Lindorff-Larsen, K.; Piana, S.; Dror, R. O.; Eastwood, M. P.; Bank, J. A.; Jumper, J. M.; Salmon, J. K.; Shan, Y.; Wriggers, W. *Science* **2010**, *330*, 341−346.
(31) Freddolino, P. L.; Park, S.; Roux, B.; Schulten., K. *Biophys. J.* **2009**, *96*, 3772−3780.
(32) Warshel, A.; Kato, M.; Pisliakov, A. V. *J. Chem. Theory Comput.* **2007**, *3*, 2034−2045.
(33) Ji, C. G.; Mei, Y.; Zhang, J. Z. H. *Biophys. J.* **2008**, *95*, 1080−1088.
(34) Ji, C. G.; Zhang, J. Z. H. *J. Am. Chem. Soc.* **2008**, *130*, 17129−17133.
(35) Duan, L. L.; Mei, Y.; Zhang, Q. G.; Zhang, J. Z. H. *J. Chem. Phys.* **2009**, *130*, 115102.
(36) Ji, C. G.; Zhang, J. Z. H. *J. Phys. Chem. B* **2009**, *113*, 16059−16064.
(37) Ji, C. G.; Zhang, J. Z. H. *J. Phys. Chem. B* **2009**, *113*, 13898−13900.
(38) Tong, Y.; Ji, C. G.; Mei, Y.; Zhang, J. Z. H. *J. Am. Chem. Soc.* **2009**, *131*, 8636−8641.
(39) Tong, Y.; Mei, Y.; Li, Y. L.; Ji, C. G.; Zhang, J. Z. H. *J. Am. Chem. Soc.* **2010**, *132*, 5137−5142.
(40) Xie, W.; Orozco, M.; Truhlar, D. G.; Gao, J. *J. Chem. Theory Comput.* **2009**, *5*, 459−467.
(41) Myers, J. K.; Pace, C. N. *Biophys. J.* **1996**, *71*, 2033−2039.
(42) Duan, L. L.; Mei, Y.; Zhang, D. W.; Zhang, Q. G.; Zhang, J. Z. H. *J. Am. Chem. Soc.* **2010**, *132*, 11159−11164.
(43) Uceda, D. P.; Pastor, M. T.; Salgado, J.; Lucena, A. P.; Payá, E. P. *J. Pept. Sci.* **2008**, 845−854.
(44) Lin, E.; Shell, M. S. *J. Chem. Theory Comput.* **2009**, *5*, 2062−2073.
(45) Onufriev, A.; Bashford, D.; Case, D. A. *J. Phys. Chem. B* **2000**, *104*, 3712−3720.
(46) Kim, E.; Jang, S.; Pak, Y. *J. Chem. Phys.* **2008**, *128*, 175104.
(47) Cornell, W. D.; Cieplak, P.; Bayly, C. I.; Kollman., P. A. *J. Am. Chem. Soc.* **1993**, *115*, 9620−9631.
(48) Onuchic, J. N.; Wolynes, P. G. *Curr. Opin. Struct. Biol.* **2004**, *14*, 70−75.
(49) Swaminatban, S.; Harte, W. E. Jr; Beveridge, D. L. *J. Am. Chem. Soc.* **1991**, *113*, 2717−2721.
(50) Hunenberger, P. H.; Mark, A. E.; van Gunsteren, W. F. *J. Mol. Biol.* **1995**, *252*, 492−503.
(51) Arnold, G. E.; Ornstein, R. L. *Biophys. J.* **1997**, *73*, 1147−1159.
(52) Estabrook, R. A.; Luo, J.; Purdy, M. M.; Sharma, V.; Weakliem, P.; Bruice, T. C.; Reich, N. O. *Proc. Natl. Acad. Sci. U.S.A.* **2004**, *102*, 994−999.
(53) Ghosh, A.; Vishveshwara, S. *Proc. Natl. Acad. Sci. U.S.A.* **2007**, *104*, 15711−15716.
(54) McCammon, J. A.; Harvey, S. C. *Dynamics of Proteins and Nucleic Acids*; Cambridge University Press: Cambridge, U.K., 1988.
(55) Hilser, V. J.; Freire, E. *Proteins: Struct., Funct., Genet.* **1997**, *27*, 171−183.
(56) Bu, Z.; Cook, J.; Callaway, D. J. *J. Mol. Biol.* **2001**, *312*, 865−873.
(57) Pearlman, D. A.; Case, D. A.; Caldwell, J. W.; Ross, W. S.; Cheatham, T. E. III; DelBolt, S.; Ferguson, D.; Seibel, G.; Kollman, P. *Comput. Phys. Commun.* **1995**, *91*, 1−41.
(58) Pastor, R. W.; Brooks, B. R.; Szabo, A. *Mol. Phys.* **1988**, *65*, 1409−1419.
(59) Ryckaert, J. P.; Ciccotti, G.; Berendsen, H. J. C. *J. Comput. Phys.* **1977**, *23*, 327−341.